Construction and Building Materials 141 (2017) 94–103

Contents lists available at ScienceDirect

Construction and Building Materials

journal homepage: www.elsevier.com/locate/conbuildmat

# Effect of triethanolamine on cement hydration toward initial setting time

Yohannes L. Yaphary [a,b], Zechuan Yu [a], Raymond H.W. Lam [b], Denvid Lau [a,c,*]

[a] Department of Architecture and Civil Engineering, City University of Hong Kong, Hong Kong, China
[b] Department of Mechanical and Biomedical Engineering, City University of Hong Kong, Hong Kong, China
[c] Department of Civil and Environmental Engineering, Massachusetts Institute of Technology, Cambridge, MA 02139, USA

## HIGHLIGHTS

- Experiments are conducted to examine the effect of TEA toward initial setting time of hydrated cement.
- Working principles of accelerated $C_3A$ hydration and ettringite formation are discussed.
- Accelerating-retarding effects of TEA on initial setting time of hydrated cement are examined.

## GRAPHICAL ABSTRACT

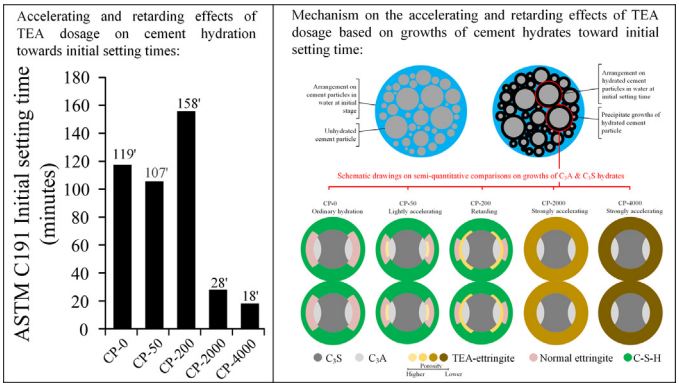


## ARTICLE INFO

*Article history:*
Received 18 September 2016
Received in revised form 17 January 2017
Accepted 15 February 2017

*Keywords:*
Additive
Cement hydration
Initial setting time
Triethanolamine

## ABSTRACT

The present study investigates the working principle upon the accelerating-retarding effect of triethanolamine dosage on the initial setting time of hydrated cement. We have conducted atomistic simulation to probe the molecular interactions between triethanolamine and dissolved ions of hydrated cement and have performed experiment to examine the effect of triethanolamine upon cement hydration. It is found that the accelerating-retarding effect of triethanolamine on the initial setting time is caused by the different intensity of formed ettringite, which is governed by the triethanolamine dosage. This finding provides the piece of insight information on the roles of triethanolamine and ettringite formation upon the initial setting time.



## 1. Introduction

In applications of cement based materials, initial setting time is the main parameter governing the operation schedule for transporting, placing, consolidating and finishing processes of concrete [1–3]. Initial setting time which is beyond the specification can jeopardize the workability for proper placing and the progress of construction schedule. Control over the initial setting time starts from the cement production process. During this process, the sample of cement is taken frequently for finding the initial setting time. The standard test method ASTM C191 is adopted by most cement producing plants to determine the initial setting time. The most viable approach to control initial setting time is to incorporate chemical additive into cement during the comminution process. There are numerous selections in the market for the chemical

* Corresponding author at: Department of Architecture and Civil Engineering, City University of Hong Kong, Hong Kong, China.
*E-mail address:* denvid@mit.edu (D. Lau).

http://dx.doi.org/10.1016/j.conbuildmat.2017.02.072
0950-0618/

additive that can be incorporated into cement based materials to influence setting time. The chemical additive can be grouped based on the typical applications, *i.e.*, normal [4], shotcrete [5,6] and cement comminution process [7,8]. Normally, those accelerators are used to shorten the setting time. In shotcrete and cement comminution process, the accelerator family is designed with additional features to enhance adhesiveness and cohesiveness (*e.g.* to reduce shotcrete rebound) and to improve the comminution efficiency respectively. The accelerator, which is alkali and chloride free, is preferable. Alkali can cause health issue and chloride induces corrosion in steel reinforcement [9,10]. We arrange the accelerator family with the chemical examples, as presented in Table 1 [11–13].

Triethanolamine (TEA) is the main chemical used as cement additive with multi functions as grinding aid during cement comminution process and setting time regulator for cement hydrations. This couple function is the main advantage from using TEA in addition to the relatively small dosage as well as the alkali and chloride free features. A unique characteristic of TEA is that it can either accelerate or retard cement hydration toward initial setting time depending on the dosage used [14–17]. TEA is respectively identified as light accelerator, retarder and strong accelerator in the typical magnitudes of dosages 200 ppm, 5000 ppm and 10,000 ppm [18–20].

Research studies have been performed to examine the effects of TEA on hydration of cement. Strong accelerating effect on initial setting time caused by relatively high dosages of TEA has been discussed and ascribed to ettringite formation during accelerated tricalcium aluminate ($C_3A$, $3CaO{\cdot}Al_2O_3$) hydration [20]. The studies involving dosages between 1000 ppm and 10,000 ppm show that TEA accelerates the hydration of $C_3A$ as well as the formation of ettringite in the $C_3A$-gypsum-water system but retards $C_3S$ hydration [21–23]. The presence of $C_3A$, either alone or along with gypsum, largely eliminate the retarding effect on $C_3S$ hydration [23]. It means that TEA mainly influences $C_3A$ during cement hydration in which $C_3A$ and gypsum exist. Studies at molecular levels shows that TEA interacts with metal ions (*e.g.* $Fe^{3+}$, $Al^{3+}$ and $Ca^{2+}$) in the pore solution of hydrated cement [24–26]. The chelating metal ions ($Fe^{3+}$ and $Al^{3+}$) by TEA possibly cause the accelerated $C_3A$ hydration. TEA chelates calcium ions ($Ca^{2+}$) and changes the morphology of formed portlandite. The chelation mechanism of amino alcohols such as TEA with metal ions is based on complexation reaction, wherein amino alcohols act as an electron pair donor [27,28]. It is noticed that TEA chelates different types of metal ions appearing at different stages of cement hydration. Apart from the understanding upon the chelating effects of TEA with metal ions dissolved from cement hydration, the working principle of TEA to control initial setting time is still not fully understood. More specifically, the working principle regarding light acceleration and retardation effects of TEA dosages on initial setting time are still missing. This working principle can provide the essential information for optimizing the use of TEA to control initial setting time.

**Table 1**
Setting time accelerating chemical additive.

| Typical application | Family | Examples of chemical | Dosage range (bwc) |
|---|---|---|---|
| Normal | Chloride | Calcium chloride | ~2% |
| | Chloride free | Calcium nitrate, lithium salts, calcium formate | 0.5–6% |
| Shotcrete | Alkaline | Aluminate bases, sodium silicate | 2–4% |
| | Alkaline-free | Aluminum sulfate | 5–11% |
| Cement comminution | Cement grinding aid | TEA | Up to 0.5% (5000 ppm) |

The aim of present study is to gain a comprehensive insight of TEA in regulating the initial setting time of hydrated cement. In particular, this study provides the working principle for the accelerating-retarding effects toward the initial setting time of cement hydration in the presence of TEA. Noteworthy, the found working principle provides the information on the technique to control the cement hydration toward the initial setting time.

The scope of the present study is the examination of cement hydration with respect to the effect of TEA with different dosages on initial setting time. Herein, we involve both experiments and atomistic simulation. On one hand, we firstly performed the tests to find accelerating and retarding effects of TEA dosages on initial setting time of hydrated cement. Subsequently, exothermic temperature of hydrated cement was monitored to examine the variation in cement hydration with different dosages of TEA. Next, examination on the change in dissolution and precipitation of hydrated cement with TEA was investigated through Fourier transform infrared (FTIR) and thermogravimetric analysis (TGA). On the other hand, atomistic simulation is conducted to probe the interactions between TEA molecules with dissolved ions of hydrated cement. Finally, based on the results from experiments and atomistic simulation, we discover the working principle for the effects of TEA dosages on the initial setting time.

## 2. Experiments

### 2.1. Materials

Materials used in this study were ASTM C150 type 1 cement, distilled water and TEA solution 85% produced by Horizon Chemical Company Limited. ASTM C204 fineness of cement is 349 $m^2/kg$ as obtained from manufacturer specification and no additive was used. The cement used for all the tests was taken from the same commercial 45 kg bag to minimize the variation of cement. The content of calcium silicates is 77% for this cement with the main chemical composition is shown in Table 2.

### 2.2. Methods

Mixing of cement paste followed the procedure of ASTM C187. The composition of cement paste in all specimens was cement 650 g and water 160 g which met the normal consistency as defined in ASTM C187. TEA dosages of specimens were 50 ppm, 100 ppm, 200 ppm, 1000 ppm, 2000 ppm, 3000 ppm and 4000 ppm by weight of cement. A lower concentration in the dosage range (*i.e.* 50 ppm–4000 ppm) was initially chosen based on the reported dosage in literature for CGA and we simultaneously increased the dosage to cover the accelerating-retarding effects of cement on the initial setting [29]. In order to incorporate TEA into specimens, TEA solution 85% was first diluted into TEA solution 10% for more accurate weighing. Afterward, TEA solution 10% was put into the mixing water of each cement paste with its specified TEA dosage. The water in TEA solution was accounted to make the total amount of water in each specimen to be 160 g. Balance with accuracy ±0.01 g was used to weigh TEA. This accuracy gave the maximum error 2 ppm of TEA dosage (in the range 50 ppm–4000 ppm) incorporated into the cement paste.

Test on initial setting time followed the procedure in ASTM C191. This test aimed to select the specimen that represented the hydrated cement with lightly accelerated, retarded and strongly accelerated initial setting time. Over the selected specimens, exothermic temperature, FTIR and TGA tests were performed.

**Table 2**
Main chemical composition of cement used in present study, ASTM C150 type 1 with ASTM C204 fineness 349 $m^2$/kg.

| Chemical | CaO | $SiO_2$ | $Al_2O_3$ | $Fe_2O_3$ | MgO |
|---|---|---|---|---|---|
| Percentage | 65.7% | 21.6% | 5.6% | 3.2% | 2.0% |

The exothermic reaction of cement hydration was followed by measuring the temperature change of cement hydration as the same approach was used in the previous study [16]. The temperature measurement of the cement paste was measured with thermocouple connected to a real-time data logger and was started within 15 s after mixing. This temperature measurement was performed for 600 min after mixing to cover acceleration period of cement hydration with various TEA dosages. Then, FTIR spectrum was acquired utilizing Bruker Tensor 27 FTIR Spectrometer. First spectrum of each specimen was obtained as early as 15 min after mixing the cement paste. Attenuated total reflectance (ATR) was used that allowed the FTIR analysis to run without prior sample preparations. Next, TGA was performed using thermal analyzer at the initial setting time of each specimen. The heating rate was 10 °C $min^{-1}$ when the temperature was between 40 °C and 1000 °C. The flow rate of argon was 100 ml $min^{-1}$ and the sample mass was 20 mg. The ambient temperature in which the materials stored and the tests performed was 21.0 ± 0.5 °C.

### 2.3. Specimen nomenclature

Throughout the present study, the nomenclature for specimen of cement paste is in the form of abbreviation of cement paste (CP) and the respective TEA dosage in ppm by weight of cement, *i.e.* CP-50, CP-100, CP-200, CP-1000, CP-2000, CP-3000 and CP-4000.

## 3. Atomistic simulation

Atomistic simulation techniques are powerful to probe cement hydration at the nanoscale [30–37]. Among them, the *ab initio* approach is appropriately useful to predict chemical reactions based on the electronic configurations of reactants. Here, we employ density functional theory (DFT) to evaluate the interaction between dissolved $C_3A$ and TEA. We refer to literally available knowledges on dissolution of $C_3A$ and perform a series of atomistic simulations to examine the $C_3A$ hydration with TEA.

At the beginning of cement hydration, complex chemical reactions occur, mainly involving $C_3A$ and gypsum. Gypsum releases $Ca^{2+}$ and $SO_4^{2-}$ following Eq. (1) [38,39]. $C_3A$ releases $Al(OH)_4^-$ and $OH^-$ following the reaction in Eq. (2). After chemical reactions, the dissolved ions from gypsum and $C_3A$ precipitate to form ettringite following Eq. (3). Ettringite has chemical formula $Ca_6Al_2(SO_4)_3(OH)_{12}{\cdot}26H_2O$ [40].

$$3CaSO_4 \cdot 2H_2O + 1.5OH^- \rightarrow 1.5Ca^{2+} + 1.5Ca(OH)^{2+} + 3SO_4^{2-} + 2H_2O \quad (1)$$

$$C_3A + 6H_2O \rightarrow 2Al(OH)_4^- + 8OH^- + 3Ca^{2+} \quad (2)$$

$$3Ca^{2+} + 3CaOH^+ + 2Al(OH)_4^- + 3SO_4^{2-} + 2.5OH^- + 26H_2O \rightarrow Ettringite + 1.5OH^- \quad (3)$$

It is inferred that the $Al(OH)_4^-$ can react with TEA to form TEA-Al complex $(OH)Al(OCH_2CH_2)_3N^-$ following Eq. (4) [41,42], where the chemical formula $(HOCH_2CH_2)_3N$ refers to TEA.

$$(HOCH_2CH_2)_3N + Al(OH)_4^- \rightarrow (HO)Al(OCH_2CH_2)_3N^- + 3H_2O \quad (4)$$

The feasibility for spontaneous reaction of Eq. (4) can be evaluated according to electronic structures as well as the total energy difference between the two sides. DFT calculations are performed to calculate the potential energy of each component with the NWChem code [43]. Geometry optimization and energy calculation are performed using B3LYP functional with the basis set 6-31G* [44–48]. Solvation effects are simulated with the COSMO model [49,50]. Initial structures of TEA and TEA-Al are obtained from the existing studies [41,42]. Initial structure of aluminate aqueous anion is based on a tetrahedral structure with Al-O distance of 1.792 Å [51]. Output information include the molecular orbitals and total energy of individual molecule involved in Eq. (4). A good agreement is observed between the optimized molecular structures obtained from our calculations and existing studies [41,42].

## 4. Results and discussions

Firstly, accelerated $C_3A$ hydration and ettringite formation with TEA are discussed based on the result of atomistic simulation. Then, we describe how the behavior of hydrated cement changes with different TEA dosages from the experimental perspective and we focus on four aspects, namely (1) initial setting time, (2) temperature evolution curve, (3) FTIR spectrum and (4) TGA curve. At the end of this section, the working principle of TEA effects on the initial setting time of hydrated cement is discussed.

### 4.1. Atomistic simulation on $C_3A$ hydration with TEA

The DFT calculations reveal the electron structures of the reactants and compute the energy difference for evaluating the spontaneity of the chemical reaction in Eq. (4). The highest occupied molecular orbital (HOMO) of aluminate aqueous anion and the lowest unoccupied molecular orbital (LUMO) of TEA are plotted in Fig. 1a and b, respectively. The HOMO of $Al(OH)_4^-$ shows three dense electronic clouds located around the oxygen atoms, indicating that $Al(OH)_4^-$ can act as nucleophiles. Meanwhile, the LUMO of TEA shows dense electronic clouds capping over the distal hydrogen atoms and the middle nitrogen atom, implying the electrophilic sites. Successively, the HOMO in $Al(OH)_4^-$ and LUMO in TEA are likely to overlap forming a TEA-Al complex as shown in Fig. 1c.

The total energy of each component in chemical reaction in Eq. (4) is listed in Table 3. The difference in total DFT energy between two sides of reactions in Eq. (4) is −7.5 kcal/mol, with the energy lower at the products side of the reaction. This result indicates that the chemical reaction in Eq. (4) can spontaneously occur in a system containing TEA and $Al(OH)_4^-$ to form $(HO)Al(OCH_2CH_2)_3N^-$.

Eq. (4) gives additional chemical reaction that consumes the dissolved $Al(OH)_4^-$ ions from $C_3A$ hydration. This process implies the working principle of accelerated $C_3A$ hydration. In Eq. (4) dosage of TEA acts as the limiting reactant, meaning that the ettringites are must formed in two distinct conditions differentiated based on the availability of TEA. The first condition is when TEA available. The second condition is in the period when all TEA are consumed. Through the following discussions the ettringites formed under first and second conditions are accordingly named TEA-ettringite and normal ettringite. The influences of TEA make TEA-ettringite formations faster than those of normal-ettringite [21].

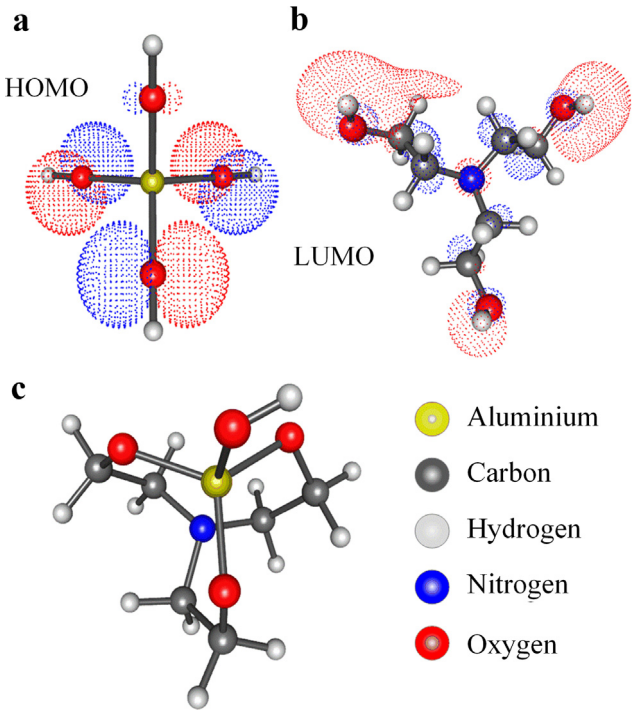


**Fig. 1.** (a) HOMO of $Al(OH)_4^-$. (b) LUMO of $(HOCH_2CH_2)_3N$. (c) The structure of $(HO)Al(OCH_2CH_2)_3N^-$. The red and blue isosurfaces indicate positive and negative values, respectively. (For interpretation of the references to colour in this figure legend, the reader is referred to the web version of this article.)

**Table 3**
The total DFT energy of each component in chemical reaction Eq. (4).

| Component | Total DFT energy (kcal/mol) |
|---|---|
| $(HOCH_2CH_2)_3N$ | −325077.3 |
| $Al(OH)_4^-$ | −342677.0 |
| $(HO)Al(OCH_2CH_2)_3N^-$ | −523889.7 |
| $H_2O$ | −143872.1 |

### 4.2. Initial setting time

The same trend for the effects of TEA dosages on initial setting time are found from previous studies [16,17,20]. This trend shows accelerating effect occur at relatively low and high dosages of TEA and in between these dosages retarding effect is observed. We confirm the trend on such effects of TEA dosages as shown in Fig. 2. The accelerating-retarding effects on initial setting time are observed in TEA dosage range 50 ppm–4000 ppm. Initial setting times of specimens CP-50 is lightly accelerated, CP-100, CP-200 and CP-1000 are retarded, and CP-2000, CP-3000 and CP-4000 are strongly accelerated, relatively to initial setting time of CP-0.

In accordance to the objective of present study, five specimens CP-0, CP-50, CP-1000, CP-2000 and CP-4000 were selected for further examination on their cement hydration. Specimen CP-0 was regarded as control. The other four specimens were used to study the effects of TEA dosages on cement hydration where initial setting time is lightly accelerated (*i.e.* CP-50), retarded (*i.e.* CP-1000) and strongly accelerated (*i.e.* CP-2000 and CP-4000).

### 4.3. Exothermic temperature

Measurement on exothermic temperature on specimens CP-0, CP-50, CP-200, CP-2000 and CP-4000 was performed to examine

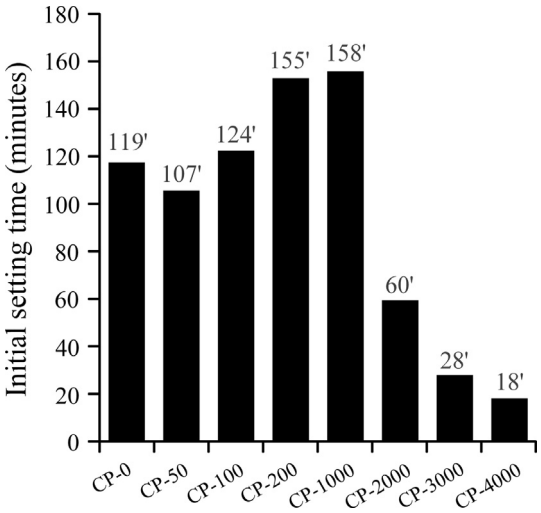


**Fig. 2.** Initial setting time as determined per ASTM C191 of ASTM C150 type 1 cement pastes with different dosages of TEA. Specimens CP-50, CP-200, CP-2000 and CP-4000 are selected to represent the cement paste experiencing the initial setting time to be lightly accelerated, retarded and strongly accelerated, respectively.

the change in reaction of cement hydration with TEA. The results are shown in Fig. 3.

In ordinary cement represented by specimen CP-0, the initial setting time occurs at early acceleration period which the start of it is defined by the length of induction period (period of slow reaction) [52] as shown from temperature evolution curve in Fig. 3a. During the induction period, the hydration of all the clinker minerals progresses relatively very slowly compared to fast hydration during preexisting induction and following acceleration periods [53]. The first and second peaks in the curves of exothermic temperatures are respectively related to the hydrations of $C_3A$ and $C_3S$ phases. The induction period in cement hydration is attributed to $C_3S$ hydration. The most possible explanations for the existence of induction period are inhibiting layer theory and "geochemical" theory of dissolution [54–57]. Inhibiting layer theory states the rapid formation of a continuous thin metastable layer of calcium silicate hydrate that effectively passivates the $C_3S$ surface layer, restricting its access to water and detaching ions away from the surface [58–60]. Recently, it is found that the "geochemical" theory of dissolution has more coincidences with experimental evidences over the inhibiting layer theory [61]. The dissolution theory states that the degree of under saturation in the solution simply governs the dissolution rate of $C_3S$. According to dissolution theory, induction period occurs due to the reach of critical degree of under saturation that dramatically slows down the rate of $C_3S$ dissolution. The dramatically slowing dissolution rate of $C_3S$ appears when the degree of under saturation is in several orders of magnitude from the equilibrium solubility. Beyond the end of induction period, which is the start of acceleration period, oriented C-S-H "needles" starts to grow on the original cement grains. Eventually, dense inner product of C-S-H start grows in between the preformed C-S-H "needles" and original cement grain [62]. C-S-H most likely only precipitates in an area close to the surface of $C_3S$ defined as reaction zone [63]. Both theories can explain the growth of C-S-H at the start of acceleration period [64]. As mentioned earlier, the first peak in exothermic temperature curve of cement hydration is attributed to $C_3A$ hydration. In cement hydration, $C_3A$ hydrates with the presence of calcium sulfate to form ettringite [61]. At early age of cement hydration, both C-S-H and ettringite precipitates are observed by scanning electron microscopy to deposit on the surface of unhydrated cement grains [65].

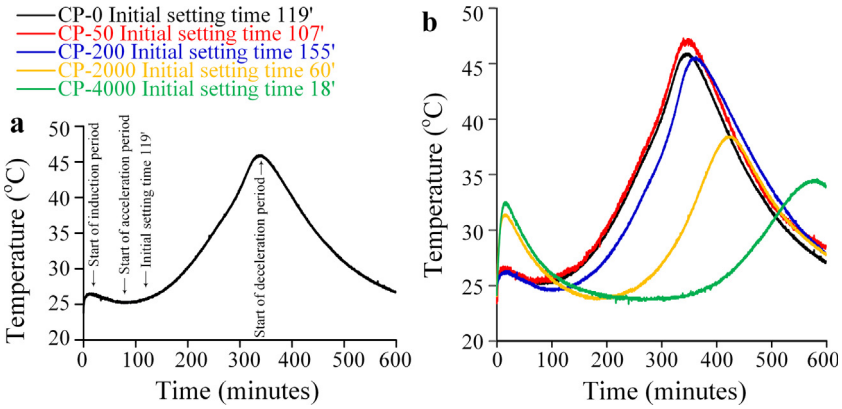


**Fig. 3.** Exothermic Temperature of hydrated cement measured up to 600 min after the start of mixing as per ASTM C187. (a) Ordinary cement. The arrows show the time of initial setting and the starts of induction, acceleration and deceleration periods of cement hydration. (b) Cements with TEA as relative to ordinary cement.

TEA changes the cement hydration as can be observed from the curves of exothermic temperatures in Fig. 3b. In specimen CP-50, the length of induction period is shortened and the start of acceleration period appears slightly earlier. Conversely, the occurrences of these two periods, accordingly, are lengthened and delayed in specimens CP-200, CP-2000 and CP-4000. Further observed distinctions, initial setting times of specimens CP-2000 and CP-4000 do not occur during the early start of acceleration as perceived in specimen CP-0, CP-50 and CP-200. Initial setting times of specimens CP-2000 and CP-4000 occur prior to starts of acceleration periods.

The intense first peak in exothermic temperature curves and the fast initial settings of specimens CP-2000 and CP-4000 are similar to the concept of "flash setting". Flash setting refers to a special setting behavior in which aluminate hydrates are formed rapidly and silicate phase hydration is retarded [25]. Improper amount of calcium sulfate causes flash setting in hydrated cement. Gypsum is the most used source of calcium sulfate. The normal initial setting of specimen CP-0 indicates the cement in present study has proper amount of calcium sulfate. Therefore, it is confirmed that the accelerating effect in specimens CP-2000 and CP-4000 is caused by TEA and is not due to improper amount of calcium sulfate.

### 4.4. Fourier transform infrared

FTIR was utilized to investigate the insight changes in the precipitation of cement hydration process with TEA. FTIR spectrums of non-hydrated cement particles, distilled water and TEA solutions with 10% and 85% concentrations are shown in Fig. 4a. In the spectrum of non-hydrated cement, absorption bands 920 $cm^{-1}$ and 1150 $cm^{-1}$ correspondingly associate with silicate, sulfate and carbonate [66–69]. In spectrums of distilled water, hydrated cement and TEA solution 10% the band is observed at 3300 $cm^{-1}$, 2200 $cm^{-1}$ and 1700 $cm^{-1}$. These bands are caused by water molecule [70,71]. In spectrum of TEA solution 85%, the very intense band appears at 1030 $cm^{-1}$. The other bands at 1120 $cm^{-1}$ and 1200 $cm^{-1}$ correspond to N-C stretch in N-$CH_2$ and C-C stretch in $CH_2$-$CH_2$, respectively [72]. The band at 2200 $cm^{-1}$ does not appear in TEA solution 85% and the band at 1030 $cm^{-1}$ is relatively less intense in TEA solution 10%, which is related to the concentration of TEA solution. In TEA solution 10%, the spectrum of water is more dominant than TEA spectrum and it is vice versa in TEA solution 85%. TEA concentration is even lesser in the specimens of cement pastes containing TEA, which cause TEA spectrum is not appear in the spectrum of hydrated specimens with TEA as shown in Fig. 4b–d.

In the spectrum of hydrated specimens, the band 660 $cm^{-1}$ appears started at 15 min for specimens CP-0, CP-50 and CP-200 shown in Fig. 4b and d. This indicates the formation of early age C-S-H that has low $CaO/SiO_2$ molar ratio (C/S). The 660–670 $cm^{-1}$ band of C-S-H due to Si–O–Si bending broadens and decreases in intensity for samples with C/S > 0.88 [73]. C/S evolves toward 1.7 for C-S-H phase in mature hydrated $C_3S$ [53]. During the short hydration period, the C-S-H formed at the surface of $C_3S$ is less than 10 nm [53]. Such formed C-S-H has very low C/S as measured using the method secondary neutral mass spectroscopy (SNMS) [53]. The observable upward shift for the FTIR spectrum between band 600 $cm^{-1}$ and 800 $cm^{-1}$ of specimens CP 2000 and 4000 (the specimens with strongly acceleration effect upon initial setting time) in Fig. 4d is due to the dominancy of the formed AFt/ettringite at the time of initial setting time as the result of relatively higher dosage of TEA. This observation coincides with the missing C-S-H band 660 $cm^{-1}$ from the FTIR spectrum. The peak at band 617 $cm^{-1}$ appearing in the FTIR spectrum of specimen with low dosage of TEA, shifting to 627 $cm^{-1}$ and sharping in the specimens with higher dosage of TEA corresponds to Al-O bond of alumatrane, which suggests the more intense quantity formation of alumatrane as higher TEA dosage [74]. More detailed observation on the sulfate band (1100–1150 $cm^{-1}$) of hydrated cements at initial setting time as shown in Fig. 4e shows the shifts to lower wavenumber that is related to formation of ettringite [67].

The intensity of early age C-S-H band at 660 $cm^{-1}$ decreases as higher TEA dosages and does not appear for specimens CP-2000 and CP-4000 (Fig. 3b-d). This indicates C-S-H formed in specimens CP-0, CP-50 and CP-200 but most likely does not in specimens CP-2000 and CP-4000 at the time of initial setting. This complies with the observation from exothermic temperature curves of specimens CP-2000 and CP-4000. The acceleration period of these two specimens, which is the indicator for the start of C-S-H formation begin beyond the time of initial setting. The shift of sulfate band to lower wavenumber from specimens CP-0 to CP-4000 (Fig. 4e) indicates the ettringite formations that tends to increase as higher TEA dosages.

### 4.5. Thermogravimetric analysis

TGA was performed to obtain more quantitative information on the precipitates formed at the time of initial setting time. Thermogravimetric (TG) curves are shown in Fig. 5. TG curve of non-hydrated cement is shown in Fig. 5a. TG curves of cements hydrated up to initial setting times are presented in Fig. 5b. The differences in TG curvatures between specimen CP-0 and those with TEA are noticeably exist below 200 °C as shown in differential thermogravimetric (DTG) curves in Fig. 5c. Here, the first two peaks at 72 °C and 110 °C correspond to decomposition of ettringite and gypsum, respectively [75–77]. The reduced weight at ~105 °C from merely the ettringite decomposition is somewhat

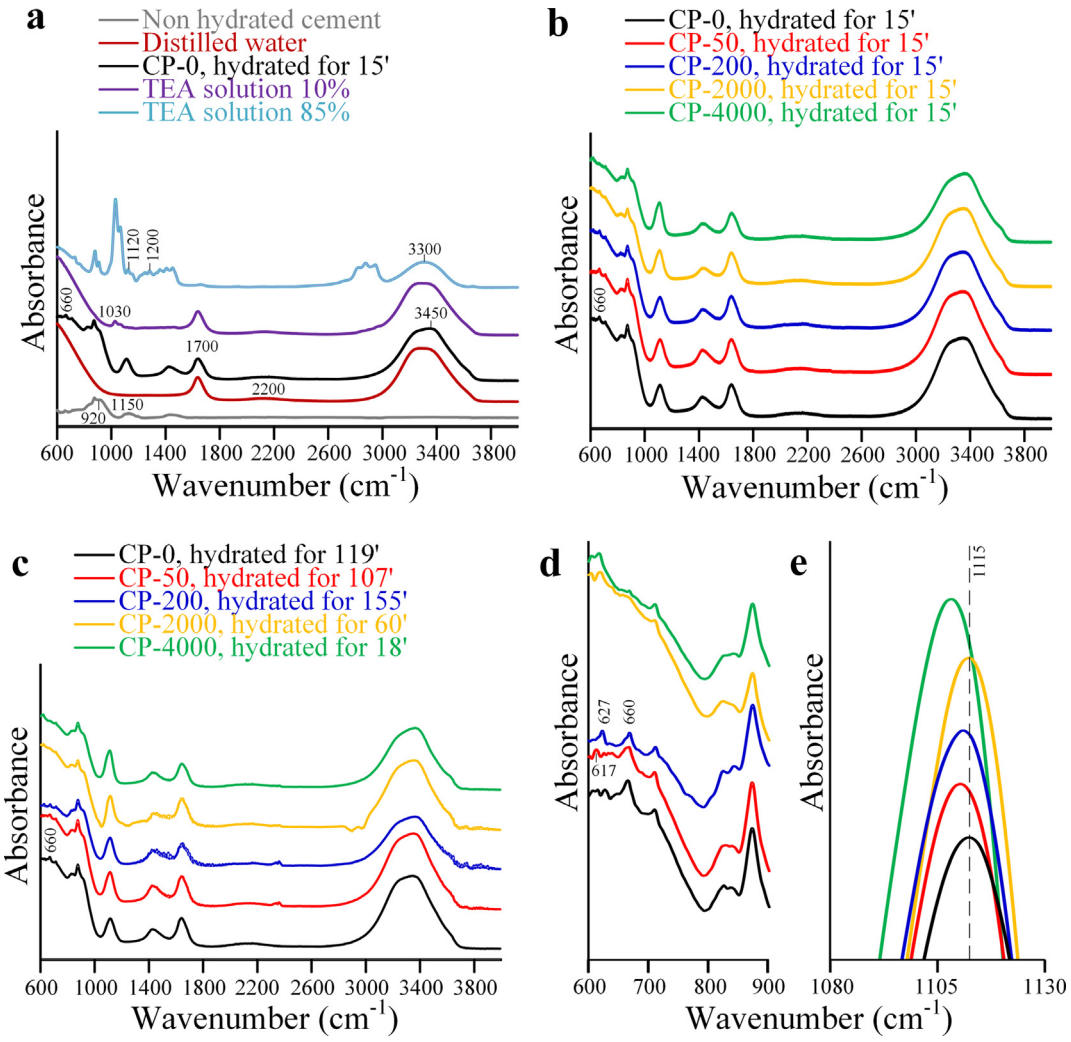


**Fig. 4.** Examination of FTIR spectrums between wavenumber 600 and 4000 $cm^{-1}$. (a) Raw materials and ordinary cement hydrated for 15 min. Hydrated cements at (b) 15 min and (c) initial setting times. Zoom in of FTIR spectrums of hydrated cements at initial setting time between the band (d) 600 and 900 $cm^{-1}$ and (e) 1080 and 1130 $cm^{-1}$. Spectrum band at 660 $cm^{-1}$ is related to low C/S C-S-H and the shift to lower wavenumber of spectrum band between 1100 and 1150 $cm^{-1}$ is related to ettringite formation.

controversial because the loss in weight also includes the water evaporation [78]. However, the weight loss due to decomposition of ettringite should be dominant, supported by the fact that ettringite starts decomposing at 50 °C and water boils above 100 °C as indicated in reference [79]. Furthermore, the evaporation time of water residing in macro-and nano- pores below 100 °C is much longer (in hours) than the time needed in the TGA test to achieve 100 °C (less than 10 min with a heating rate of 10 °C per minute). In the current study, the evaporation time of water in concrete at 100 °C would be hundreds of hours [80]. Therefore, the weight loss between 50 °C and 100 °C is used to compare the quantity of formed ettringite among the specimens. Fig. 5d presents the percentage weight loss of the specimens between 50 °C and 100 °C. The ettringite quantity is less in specimens CP-50 and CP-200 but is more in specimens CP-2000 and CP-4000 as compared to the quantity in specimen CP-0.

### *4.6. Working principle on accelerating-retarding effects of TEA dosage on initial setting time*

Atomistic simulation suggests the spontaneous reaction between TEA and $Al(OH)_4$-ions from $C_3A$ hydration to form alumatrane. The presence of alumatrane can also be observed from the band 617 $cm^{-1}$ merely appearing in the FTIR spectrum of specimen with low dosage of TEA, shifting to 627 $cm^{-1}$ and sharping in the specimens with higher dosage of TEA corresponds to Al-O bond of alumatrane [74]. The additional chemical reaction in presence of TEA that consumes the dissolved $Al(OH)_4$- ions from $C_3A$ hydration suggests the needs on faster dissolution of $C_3A$ in order to maintain the chemical equilibration in hydrated cement solution. Therefore, this process implies the working principle of accelerated $C_3A$ hydration in the presence of TEA.

Because of the relatively small dosage of TEA (only up to 4000 ppm) and the imbalance between TEA and $C_3A$, dosage of TEA acts as the limiting reactant, meaning that the ettringites are must be formed in two distinct conditions differentiated based on the availability of TEA. The first condition is with TEA available. The second condition is in the period when all TEA are consumed. Through the following discussions the ettringites formed under first and second conditions are named TEA-ettringite and normal ettringite, respectively. Though the detailed molecular structure of TEA-ettringite is worth determined in the future study, our work clearly show that TEA contributes to the more rapid TEA-ettringite formation than the normal-ettringite formation [21].

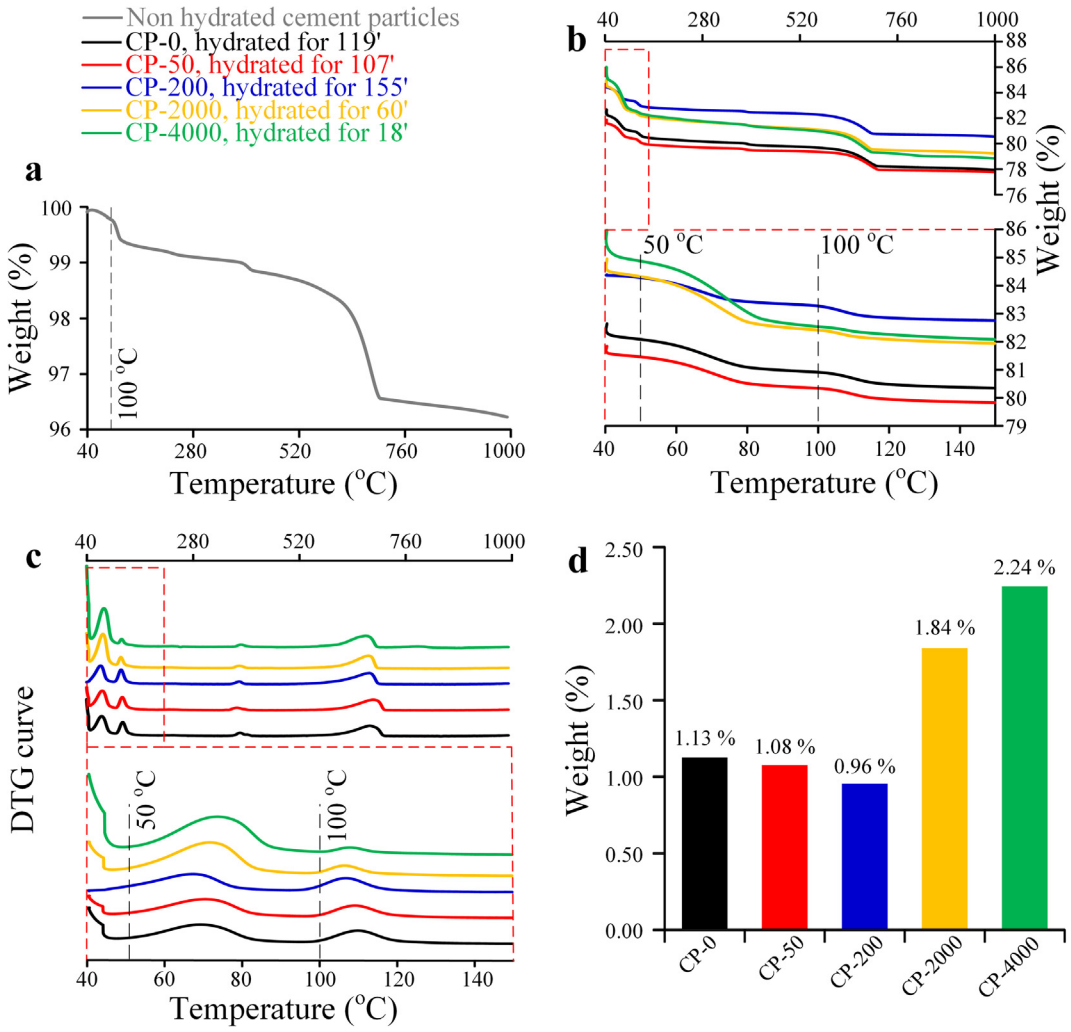


**Fig. 5.** (a) TGA of non-hydrated cement particles. (b) TGA of hydrated cements at initial setting times. (c) DTG of hydrated cements. Ettringite is decomposed between 50 °C and 100 °C. (d) % weight loss of hydrated cements between 50 °C and 100 °C which shows the quantitative comparisons of ettringite formations.

The TEA dosage governs the quantity of TEA-ettringite being formed, which subsequently influences the following cement hydration process (up to the time of initial setting) including the $C_3S$ phase. Such influence leads to lightly accelerating (low dosage), retarding (medium dosage) and strongly accelerating (high dosage) effects of TEA on the initial setting time. In the following paragraphs, we explain the working principle for the accelerating-retarding effects of TEA dosage on initial setting time. This working principle is based on the semi-quantitative comparison of the formed TEA-ettringite that leads to different effects of TEA dosage on cement hydration and initial setting time. We start with the discussions regarding the initial setting time of specimen CP-0. Subsequently, we discuss the working principles of accelerating-retarding effects of TEA dosage on initial setting time in specimens CP-50, CP-200, CP-2000 and CP-4000.

The time of initial setting of specimen CP-0 (ordinary hydrated cement) is the moment when the growths of hydration products surrounding cement particles start colliding [81,82]. These colliding hydration products form percolating solid networks over the entire hydrated cement system as illustrated in Fig. 6a. Fig. 6b gives the semi-quantitatively schematic drawing of cement particle ($C_3S + C_3A$) and the respective formed C-S-H and normal-ettringite at initial setting time. Initial setting time appears as the consequence of both $C_3S$ and $C_3A$ hydrations and the respective formations of C-S-H and ettringite [83]. Formation of C-S-H contributes more to the initial setting time as compared to ettringite.

Specimen CP-50 represents cement paste where TEA lightly accelerates the initial setting time. This lightly accelerating effect of TEA can be explained from the shorter induction period in specimen CP-50 than that in specimen CP-0. The shorter induction period in specimen CP-50 can be interpreted as the effect from the formation of TEA-ettringite on the surface of $C_3A$ that makes $C_3A$ further dissolution impeded. As the $C_3A$ hydration is impeded, less quantity of ettringites in specimen CP-50 (Fig. 6c) than CP-0 (Fig. 6b). TGA indicates the formed ettringite is less in specimen CP-50 than that in specimen CP-0. The interruption of $C_3A$ hydration after the formation of TEA-ettringite makes the solution is more relatively under saturated with respect to dissolved $C_3A$. This situation gives more opportunity for $C_3S$ to dissolve faster and C-S-H precipitates earlier hence induction period is shortened. Earlier start of acceleration period in exothermic temperature curve of specimen CP-50 than CP-0 indicates the earlier C-S-H precipitation. As the result, C-S-H network is built up faster hence initial setting time is accelerated.

Specimen CP-200 corresponds the cement paste where TEA retards the initial setting time. Similar to the case of specimen CP-50, the retardation in initial setting time of specimen CP-200 can be explained from the length of induction period. Induction

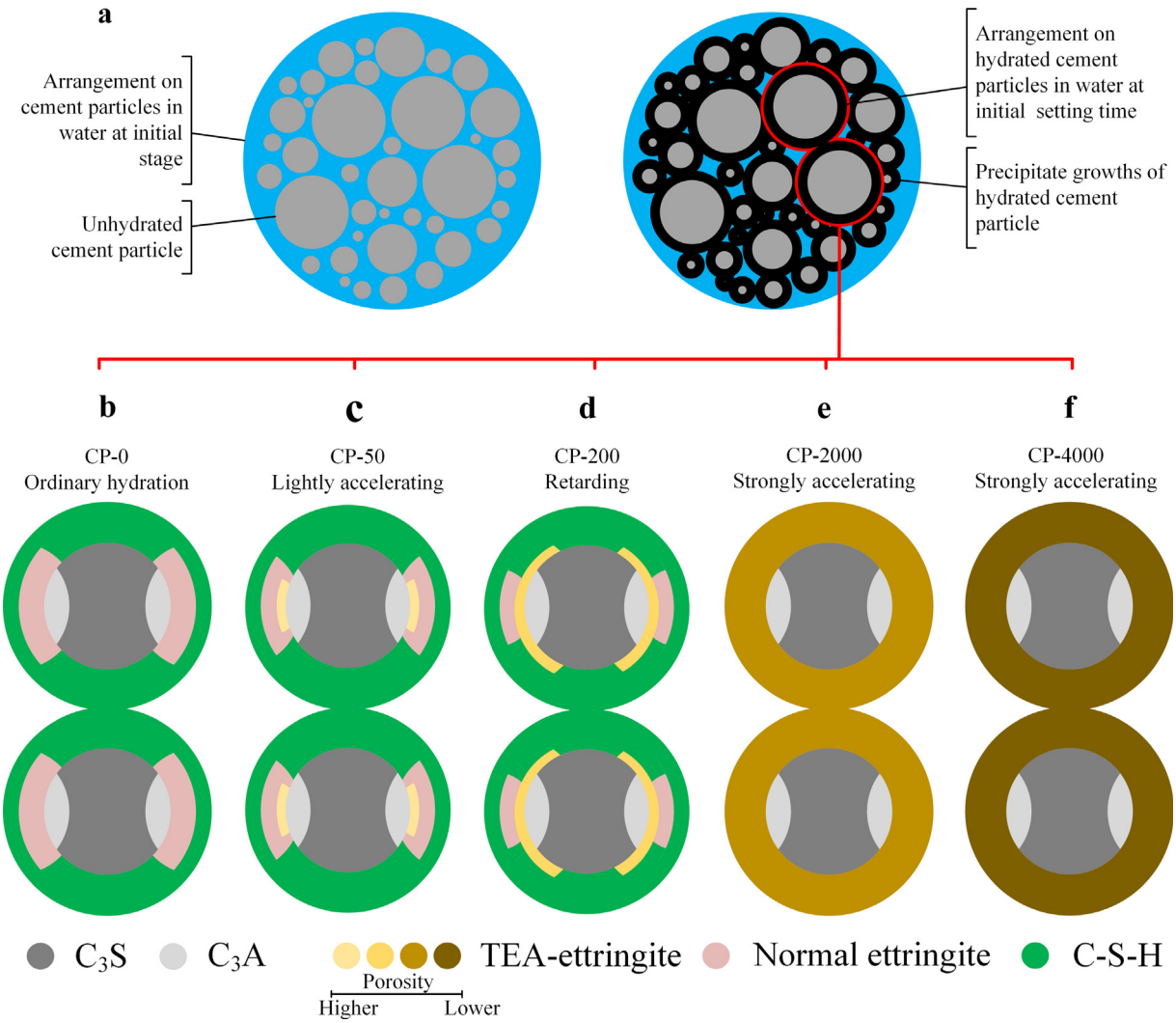


**Fig. 6.** (a) Schematic drawings show the evolution of hydrated cement particles toward initial setting time. Cement particles hydrate and their products, mainly come from the hydrations of $C_3S$ and $C_3A$ phases, grow outward the surface of non-hydrated cement particles. Initial setting time occur when the growing hydration products start to collide. (b–f) Schemes on semi-quantitative comparison of cement ($C_3S + C_3A$) hydration products at the initial setting time. (c) The intensity of formed TEA-ettringite impedes the growth of normal ettringite causing the more exposed $C_3S$ hence faster C-S-H formation to cause initial setting time. (d) Growth of TEA-ettringite on $C_3A$ and partly $C_3S$ surfaces causing slower C-S-H formations for initial setting time. In (b–d), initial setting time are developed dominantly by C-S-H formation, while in (e and f), the initial setting times are mainly ascribed to excessive amount of TEA-ettringite.

period in specimen CP-200 is longer. The more quantity of TEA-ettringite in specimen CP-200 than in specimen CP-50 can explain such longer induction period. The quantity of TEA-ettringite in specimen CP-200 is adequate to grow not only over $C_3A$ surface but also on part of $C_3S$ surface as illustrated in Fig. 6d. TEA-Ettringite on the surfaces of $C_3A$ and $C_3S$ interferes hydrations of $C_3A$ and $C_3S$. Consequently, the pace of C-S-H growth is impeded hence the occurrence of initial setting is prolonged.

Strong acceleration effect of TEA on initial setting time occurs in specimens CP-2000 and CP-4000. Exothermic temperature curves of specimens CP-2000 and CP-4000 are largely deviate from those of specimens CP-0, CP-50 and CP-200. Noticeable changes are in terms of significant higher intensities of the first peaks, long induction periods and prolonged starts of acceleration periods. Initial setting time of specimens CP-2000 and CP-4000 coincides the period of the first peak, which correspond to $C_3A$ hydration. This coincidence implies that TEA-ettringite causes initial setting time in specimens CP-2000 and CP-4000 (Fig. 6e and f). FTIR spectrum analysis indicates inexistences of C-S-H at initial setting time of specimens CP-2000 and CP-4000. Such formation of TEA-ettringite strongly impedes $C_3S$ hydration and causes the inexistences of C-S-H at initial setting time of specimens CP-2000 and CP-4000. The longer induction period in specimen CP-4000 relatives to specimen CP-2000 is most likely related to the less porosity of TEA-ettringite formed in specimen CP-2000 than that in specimen CP-4000. The less porous TEA-ettringite in specimen CP-4000 than CP-2000 gives more intense barrier between water and $C_3S$ to start hydrate. The change into the smaller size of ettringite crystals is observed in hydrated cement paste with TEA [84].

## 5. Conclusion

In this study, we have performed experiments and molecular simulation for the discovery of working principle to explain the accelerating-retarding effects of TEA dosage on initial setting time of hydrated cement. TEA initially influences $C_3A$ hydration. In the presence of TEA, $C_3A$ hydration involves the formation of alumatrane as has been evaluated by molecular simulation and FTIR spectroscopy. Under this TEA influencing circumstance, the precip-

itate called TEA-ettringite are formed. The pace of TEA-ettringite formation is faster than normal ettringite. The level in intensity of TEA-ettringite formation is governed by TEA dosage and can influence the cement hydration to different extents prior the initial setting time.

Acceleration of initial setting time of hydrated cement with considered low dosage of TEA has the acceleration period that starts earlier and with lower quantity of ettringite. These observations suggest the relatively small quantity of TEA-ettringite rapidly grows on $C_3A$ surface, which impedes the normal ettringite formation and allows the other phases of cement such as $C_3S$ to hydrate faster. Consequently, general process in cement hydration is accelerated hence initial setting time. In presence of relatively higher dosage of TEA, the amount of TEA is adequate to cause the fast network formation of TEA-ettringite that can generate initial setting time. Retardation in initial setting time from the use of TEA with considered medium dosage is caused by TEA-ettringite that adequately grows on the surfaces of $C_3A$ and other cement phases. As a consequence, the subsequent cement hydration is impeded leading to the delayed initial setting time.

The working principle discovered in this study regarding the accelerating-retarding effects on initial setting time is not merely applicable to TEA but also in general to others chemical accelerating the hydration of $C_3A$. Furthermore, it is found that control upon hydration of $C_3A$ provides the means to regulate cement hydration toward initial setting time.

## Conflict of interest

All the authors declare that they have no conflict of interest in this research.

## Acknowledgements

This research is supported by Strategic Research Grants (project# 7000540 and 7004364) and the internal matching grant (project# 9678100) by City University of Hong Kong, Hong Kong, China. The authors are grateful to the support from the Research Grants Council (RGC) in Hong Kong through the Early Career Scheme (ECS) with the Grant No. 139113.

## References

[1] H.K. Lee, K.M. Lee, Y.H. Kim, H. Yim, D.B. Bae, Ultrasonic in-situ monitoring of setting process of high-performance concrete, Cem. Concr. Res. 34 (2004) 631–640.
[2] J.-J. Zheng, J. Zhang, G.W. Scherer, Prediction of the degree of hydration at initial setting time of cement paste with particle agglomeration, Cem. Concr. Res. 42 (2012) 1280–1285.
[3] A.C. Aydin, R. Gül, Influence of volcanic originated natural materials as additives on the setting time and some mechanical properties of concrete, Constr. Build. Mater. 21 (2007) 1277–1281.
[4] C.K. Nmai, Cold weather concreting admixtures, Cem. Concr. Compos. 20 (1998) 121–128.
[5] L.R. Prudêncio, Accelerating admixtures for shotcrete, Cem. Concr. Compos. 20 (1998) 213–219.
[6] I. Toma, I. Toma, P. Rolland, Method of improving shotcrete technology, U.S. Patent No. 6,465,048, 15 October, 2002.
[7] M. Weibel, R.K. Mishra, Comprehensive understanding of grinding aids, ZKG Int. 6 (2014) 28–39.
[8] Y.L. Yaphary, R.H.W. Lam, D. Lau, Chemical technologies for modern concrete production, Modern Building Materials, Structures and Techniques, MBMST, 26-27 May, Vilnius, Lithuania, 2016.
[9] M. Sommer, F. Wombacher, T.A. Bürge, Alkali-free setting and hardening accelerator, U.S. Patent No. 6,537,367, 25 March, 2003.
[10] K.Y. Ann, H.-W. Song, Chloride threshold level for corrosion of steel in concrete, Corros. Sci. 49 (2007) 4113–4133.
[11] I. Galobardes, R.P. Salvador, S.H. Cavalaro, A. Figueiredo, C.I. Goodier, Adaptation of the standard EN 196–1 for mortar with accelerator, Constr. Build. Mater. 127 (2016) 125–136.
[12] R.P. Salvador, S.H. Cavalaro, I. Segura, A.D. Figueiredo, J. Pérez, Early age hydration of cement pastes with alkaline and alkali-free accelerators for sprayed concrete, Constr. Build. Mater. 111 (2016) 386–398.
[13] J.S. Narayanan, K. Ramamurthy, Identification of set-accelerator for enhancing the productivity of foam concrete block manufacture, Constr. Build. Mater. 37 (2012) 144–152.
[14] V.S. Ramachandran, Knovel (Firm), Concrete admixtures handbook properties, science, and technology, Building Materials Science Series, Noyes Publications, Park Ridge, N.J., U.S.A., 1995.
[15] V.S. Ramachandran, Hydration of cement—role of triethanolamine, Cem. Concr. Res. 6 (1976) 623–631.
[16] V.H. Dodson, Concrete Admixtures, Van Nostrand Reinhold, New York, 1990.
[17] I. Aiad, A.A. Mohammed, S.A. Abo-El-Enein, Rheological properties of cement pastes admixed with some alkanolamines, Cem. Concr. Res. 33 (2003) 9–13.
[18] S. Aggoun, M. Cheikh-Zouaoui, N. Chikh, R. Duval, Effect of some admixtures on the setting time and strength evolution of cement pastes at early ages, Constr. Build. Mater. 22 (2008) 106–110.
[19] Z. Heren, H. Ölmez, The influence of ethanolamines on the hydration and mechanical properties of portland cement, Cem. Concr. Res. 26 (1996) 701–705.
[20] J. Han, K. Wang, J. Shi, Y. Wang, Mechanism of triethanolamine on Portland cement hydration process and microstructure characteristics, Constr. Build. Mater. 93 (2015) 457–462.
[21] V.S. Ramachandran, Action of triethanolamine on the hydration of tricalcium aluminate, Cem. Concr. Res. 3 (1973) 41–54.
[22] V.S. Ramachandran, Influence of triethanolamine on the hydration characteristics of tricalcium silicate, J. Appl. Chem. Biotech. 22 (1972) 1125–1138.
[23] S. Ghosh, Advances in Cement Technology: Chemistry, Manufacture and Testing, CRC Press, 2003.
[24] J.-P. Perez, A. Nonat, S. Pourchet, S. Garrault, M. Mosquet, C. Canevet, Why TIPA leads to an increase in the mechanical properties of mortars whereas TEA does not, ACI Special Publ. 217 (2003) 583–594.
[25] E. Gartner, D. Myers, Influence of tertiary alkanolamines on portland cement hydration, J. Am. Ceram. Soc. 76 (1993) 1521–1530.
[26] Z. Yan-Rong, K. Xiang-Ming, L. Zi-Chen, L. Zhen-Bao, Z. Qing, D. Bi-Qin, X. Feng, Influence of triethanolamine on the hydration product of portlandite in cement paste and the mechanism, Cem. Concr. Res. 87 (2016) 64–76.
[27] D.M. Roundhill, Transition metal and enzyme catalyzed reactions involving reactions with ammonia and amines, Chem. Rev. 92 (1992) 1–27.
[28] D. Prasad, M.Z. Hoffman, Charge-transfer complexation between methyl viologen and sacrificial electron donors EDTA, triethanolamine, and cysteine, J. Phys. Chem. 88 (1984) 5660–5665.
[29] L.A. Jardine, Amine-containing cement processing additives, U.S. Patent No. 7,160,384, 9 January, 2007.
[30] D. Lau, Z. Yu, Cement modeled as poly-dispersed assemblage of disk-like building blocks, in: The 2015 World Congress on Advances in Civil, Environmental and Materials Research (ACEM15), 25-28 August, Songdo Convensia, Incheon, South Korea, 2015.
[31] D. Lau, Z. Yu, O. Buyukozturk, Mesoscale modeling of cement matrix using the concept of building block, in: 2014 MRS Fall Meeting, 30 November-5 December, Boston, MA, USA.
[32] Z. Yu, D. Lau, Nano- and mesoscale modeling of cement matrix, Nanoscale Res. Lett. 10 (2015) 173.
[33] J.J. Thomas, J.J. Biernacki, J.W. Bullard, S. Bishnoi, J.S. Dolado, G.W. Scherer, A. Luttge, Modeling and simulation of cement hydration kinetics and microstructure development, Cem. Concr. Res. 41 (2011) 1257–1278.
[34] R.J.-M. Pellenq, A. Kushima, R. Shahsavari, K.J. Van Vliet, M.J. Buehler, S. Yip, F.-J. Ulm, A realistic molecular model of cement hydrates, Proc. Natl. Acad. Sci. 106 (2009) 16102–16107.
[35] H. Manzano, J.S. Dolado, A. Ayuela, Structural, mechanical, and reactivity properties of tricalcium aluminate using first-principles calculations, J. Am. Ceram. Soc. 92 (2009) 897–902.
[36] Z. Yu, A. Zhou, D. Lau, Mesoscopic packing of disk-like building blocks in calcium silicate hydrate, Sci. Rep. 6 (2016) 36967.
[37] F. Heberling, D. Bosbach, J.-D. Eckhardt, U. Fischer, J. Glowacky, M. Haist, U. Kramar, S. Loos, H.S. Müller, T. Neumann, C. Pust, T. Schäfer, J. Stelling, M. Ukrainczyk, V. Vinograd, M. Vučak, B. Winkler, Reactivity of the calcite–water-interface, from molecular scale processes to geochemical engineering, Appl. Geochem. 45 (2014) 158–190.
[38] D. Jansen, F. Goetz-Neunhoeffer, B. Lothenbach, J. Neubauer, The early hydration of Ordinary Portland Cement (OPC): An approach comparing measured heat flow with calculated heat flow from QXRD, Cem. Concr. Res. 42 (2012) 134–138.
[39] M. Tokyay, Cement and Concrete Mineral Admixtures, CRC Press, 2016.
[40] F. Goetz-Neunhoeffer, J. Neubauer, Refined ettringite ($Ca_6Al_2(SO_4)_3(OH)_{12}$·26H$_2$O) structure for quantitative X-ray diffraction analysis, Powder Diffr. 21 (2006) 4–11.
[41] J. Pinkas, J.G. Verkade, Alumatrane, $Al(OCH_2CH_2)_3N$: a reinvestigation of its oligomeric behavior, Inorg. Chem. 32 (1993) 2711–2716.
[42] L. Fernandez, P. Viruela-Martin, J. Latorre, C. Guillem, A. Beltrán, P. Amorós, Theoretical study of oligomeric alumatranes present in the chemistry of materials from micro to mesoporous molecular sieves and alumina composites, J. Mol. Struct. (Thoechem) 850 (2008) 94–104.
[43] M. Valiev, E.J. Bylaska, N. Govind, K. Kowalski, T.P. Straatsma, H.J. Van Dam, D. Wang, J. Nieplocha, E. Apra, T.L. Windus, NWChem: a comprehensive and scalable open-source solution for large scale molecular simulations, Comput. Phys. Commun. 181 (2010) 1477–1489.

[44] A.D. Becke, Density-functional thermochemistry. III. The role of exact exchange, J. Chem. Phys. 98 (1993) 5648–5652.
[45] C. Lee, W. Yang, R.G. Parr, Development of the Colle-Salvetti correlation-energy formula into a functional of the electron density, Phys. Rev. B 37 (1988) 785.
[46] B. Miehlich, A. Savin, H. Stoll, H. Preuss, Results obtained with the correlation energy density functionals of Becke and Lee, Yang and Parr, Chem. Phys. Lett. 157 (1989) 200–206.
[47] K.L. Schuchardt, B.T. Didier, T. Elsethagen, L. Sun, V. Gurumoorthi, J. Chase, J. Li, T.L. Windus, Basis set exchange: a community database for computational sciences, J. Chem. Inf. Model. 47 (2007) 1045–1052.
[48] D. Feller, The role of databases in support of computational chemistry calculations, J. Comput. Chem. 17 (1996) 1571–1586.
[49] A. Klamt, G. Schüürmann, COSMO: a new approach to dielectric screening in solvents with explicit expressions for the screening energy and its gradient, J. Chem. Soc., Perkin Trans. 2 (1993) 799–805.
[50] D.M. York, M. Karplus, A smooth solvation potential based on the conductor-like screening model, J. Phys. Chem. A 103 (1999) 11060–11079.
[51] M. Lubin, E. Bylaska, J. Weare, Ab initio molecular dynamics simulations of aluminum ion solvation in water clusters, Chem. Phys. Lett. 322 (2000) 447–453.
[52] M.-H. Zhang, K. Sisomphon, T.S. Ng, D.J. Sun, Effect of superplasticizers on workability retention and initial setting time of cement pastes, Constr. Build. Mater. 24 (2010) 1700–1707.
[53] I. Odler, 6 - Hydration, Setting and Hardening of Portland Cement, in: P.C. Hewlett (Ed.), Lea's Chemistry of Cement and Concrete (Fourth Edition), Butterworth-Heinemann, Oxford, 1998, pp. 241–297.
[54] P. Juilland, E. Gallucci, R.J. Flatt, K.L. Scrivener, Reply to the discussion by E. Gartner of the paper "Dissolution theory applied to the induction period in alite hydration", Cem. Concr. Res. 41 (2011) 563–564.
[55] E. Gartner, Discussion of the paper "Dissolution theory applied to the induction period in alite hydration" by P. Juilland et al., Cem. Concr. Res. 40 (2010) 831–844, Cement and Concrete Research, 41 (2011) 560–562.
[56] J.M. Makar, J.J. Beaudoin, T. Sato, R. Alizadeh, L. Raki, Discussion of "Dissolution theory applied to the induction period in alite hydration", Cem. Concr. Res. 41 (2011) 565–567.
[57] P. Juilland, E. Gallucci, R.J. Flatt, K.L. Scrivener, Reply to the discussion by J. Makar, J.J. Beaudoin, T. Sato, R. Alizadeh and L. Raki of "Dissolution theory applied to the induction period in alite hydration", Cem. Concr. Res. 41 (2011) 568–569.
[58] H. Stein, J. Stevels, Influence of silica on the hydration of 3 CaO, $SiO_2$, J. Appl. Chem. 14 (1964) 338–346.
[59] H. Jennings, P. Pratt, An experimental argument for the existence of a protective membrane surrounding Portland cement during the induction period, Cem. Concr. Res. 9 (1979) 501–506.
[60] J.W. Bullard, H.M. Jennings, R.A. Livingston, A. Nonat, G.W. Scherer, J.S. Schweitzer, K.L. Scrivener, J.J. Thomas, Mechanisms of cement hydration, Cem. Concr. Res. 41 (2011) 1208–1223.
[61] K.L. Scrivener, P. Juilland, P.J.M. Monteiro, Advances in understanding hydration of Portland cement, Cem. Concr. Res. 78 (Part A) (2015) 38–56.
[62] A. Bazzoni, S. Ma, Q. Wang, X. Shen, M. Cantoni, K.L. Scrivener, The effect of magnesium and zinc ions on the hydration kinetics of $C_3S$, J. Am. Ceram. Soc. 97 (2014) 3684–3693.
[63] E. Masoero, J.J. Thomas, H.M. Jennings, A reaction zone hypothesis for the effects of particle size and water-to-cement ratio on the early hydration kinetics of C3S, J. Am. Ceram. Soc. 97 (2014) 967–975.
[64] J.W. Bullard, R.J. Flatt, New insights into the effect of calcium hydroxide precipitation on the kinetics of tricalcium silicate hydration, J. Am. Ceram. Soc. 93 (2010) 1894–1903.
[65] K.L. Scrivener, A. Nonat, Hydration of cementitious materials, present and future, Cem. Concr. Res. 41 (2011) 651–665.
[66] R. Ylmén, U. Jäglid, B.-M. Steenari, I. Panas, Early hydration and setting of Portland cement monitored by IR, SEM and Vicat techniques, Cem. Concr. Res. 39 (2009) 433–439.
[67] M.Y.A. Mollah, W. Yu, R. Schennach, D.L. Cocke, A Fourier transform infrared spectroscopic investigation of the early hydration of Portland cement and the influence of sodium lignosulfonate, Cem. Concr. Res. 30 (2000) 267–273.
[68] D. Govindarajan, R. Gopalakrishnan, Spectroscopic studies on Indian Portland cement hydrated with distilled water and sea water, Front. Sci. 1 (2011) 21–27.
[69] M. Yousuf, A. Mollah, P. Palta, T.R. Hess, R.K. Vempati, D.L. Cocke, Chemical and physical effects of sodium lignosulfonate superplasticizer on the hydration of portland cement and solidification/stabilization consequences, Cem. Concr. Res. 25 (1995) 671–682.
[70] B.L. Mojet, S.D. Ebbesen, L. Lefferts, Light at the interface: the potential of attenuated total reflection infrared spectroscopy for understanding heterogeneous catalysis in water, Chem. Soc. Rev. 39 (2010) 4643–4655.
[71] D.S. Eisenberg, W. Kauzmann, The Structure and Properties of Water, Clarendon Press, Oxford, 1969.
[72] J.S. Gaffney, N.A. Marley, D.E. Jones, Fourier Transform Infrared (FTIR) spectroscopy, in: Characterization of Materials, 2012.
[73] P. Yu, R.J. Kirkpatrick, B. Poe, P.F. McMillan, X. Cong, Structure of calcium silicate hydrate (C-S-H): Near-, Mid-, and Far-infrared spectroscopy, J. Am. Ceram. Soc. 82 (1999) 742–748.
[74] X. Wu, G. Shao, S. Cui, L. Wang, X. Shen, Synthesis of a novel $Al_2O_3$–$SiO_2$ composite aerogel with high specific surface area at elevated temperatures using inexpensive inorganic salt of aluminum, Ceram. Int. 42 (2016) 874–882.
[75] A. Peschard, A. Govin, P. Grosseau, B. Guilhot, R. Guyonnet, Effect of polysaccharides on the hydration of cement paste at early ages, Cem. Concr. Res. 34 (2004) 2153–2158.
[76] J. Bensted, S.P. Varma, Some applications of infrared and Raman spectroscopy in cement chemistry Part 3-hydration of Portland cement and its constituents, Cem. Technol. 5 (1974) 440–445. 448–450.
[77] I. Odler, S. Abdul-Maula, Possibilities of quantitative determination of the AFt-(ettringite) and AFm-(monosulphate) phases in hydrated cement pastes, Cem. Concr. Res. 14 (1984) 133–141.
[78] L.P. Singh, A. Goel, S.K. Bhattacharyya, U. Sharma, G. Mishra, Hydration studies of cementitious material using silica nanoparticles, J. Adv. Concr. Technol. 13 (2015) 345–354.
[79] I. Pane, W. Hansen, Investigation of blended cement hydration by isothermal calorimetry and thermal analysis, Cem. Concr. Res. 35 (2005) 1155–1164.
[80] H.-J. Chen, C.-W. Tang, H.-S. Peng, Feasibility of utilizing oven-drying test to estimate the durability performance of concrete, Comput. Concr. 8 (2011) 389–399.
[81] G. Ye, K. Van Breugel, A. Fraaij, Three-dimensional microstructure analysis of numerically simulated cementitious materials, Cem. Concr. Res. 33 (2003) 215–222.
[82] D.P. Bentz, E.J. Garboczi, Percolation of phases in a three-dimensional cement paste microstructural model, Cem. Concr. Res. 21 (1991) 325–344.
[83] Y. Chen, I. Odler, On the origin of portland cement setting, Cem. Concr. Res. 22 (1992) 1130–1140.
[84] J. Neubauer, F. Goetz-Neunhoeffer, U. Holland, D. Schmitt, P. Gaeberlein, M. Degenkolb, Crystal chemistry and microstructure of hydrated phases occurring during early OPC hydration, in: 12th International Congress on the Chemistry of Cement, 8-13 July, Montreal, Canada, 2007.